Int. J. Electrochem. Sci., 10 **(2015)** 5498 - 5512

International Journal of
ELECTROCHEMICAL
SCIENCE
www.electrochemsci.org

Morphological Reaction on the Different Stabilizers of Titanium Dioxide Nanoparticles

Sh.Nadzirah[*]*, K.L. Foo and, U. Hashim*

Nanostructure Lab-on-chip Research Group, Institute of Nano Electronic Engineering, Universiti Malaysia Perlis (UniMAP), 01000 Kangar, Perlis Malaysia.
[*]E-mail: shnadzirahsaa@gmail.com

Received: 11 August 2014 / *Accepted:* 16 February 2015 / *Published:* 27 May 2014

Three different stabilizers have been chosen for TiO_2 solution preparation via sol-gel method to form a resistive sensor. TiO_2 solution was prepared by mixing of ethanol as a solvent, titanium isopropoxide as a precursor and hydrochloric acid (HCl) as a stabilizer thus synthesis pH 1 aqueous solution. These TiO_2 solution preparation steps were repeated by replacing HCl with another catalysts which are acetic acid (AA) (pH 3.05) and monoethanolamine (MEA) (pH 10.4) for the second and third TiO_2 solution preparation respectively. Spin-coating technique was used to uniformly deposit TiO_2 film on silicon dioxide substrate. The deposited thin films were then annealed at various temperatures (400, 500, 600, 700 and 900 ^oC) for 30 min using annealing furnace. Finally, aluminum metal was deposited on the TiO_2 film and simple lithography method was used to fabricate electrodes. The X-ray diffraction (XRD) exhibits rutile structures are more favorable to grow on TiO_2 film synthesis with acidic solution (pH 1 and pH 3.05) even at very low temperature. Otherwise, base-solution of TiO_2 tends to synthesis anatase phase at low and average temperatures. While field emission scanning electron microscopy (FESEM) was used to observe the crystallite form also reconfirmed the crystallite size growth. The relation between film roughness, thicknes are correlated with the pH level were confirmed by atomic force microscopy (AFM). The electrical current flow through these samples with fixed voltage applied were measured and it shows the smallest current flow between the fabricated fingers is 0.96 nA which is from the lowest pH level of HCl.

Keywords: Titanium dioxide; Sol-gel process; Nanoparticles; pH stabilizer.

1. INTRODUCTION

Titanium dioxide (TiO_2) or tinania is an n-type semiconductor [1] that can be formed in three different phases; which are brookite, anatase and rutile [2-6]. Various applications can be made with the use of TiO_2 since it has high chemical and temperature stability [7]. Furthermore, it has high resistance towards acid and alkali makes it suitable for artificial bone or tooth fabrication. Since it is

biocompatible material, it safes and non-poisonous for biosensor development. Moreover, it is able to generate non-poisonous CO_2 and H_2O in some inorganic products when it decomposes organic pollutants by light [7]. These multiple applications are due to its different phases formation which believed has own special properties that make TiO_2 material has been tremendous attention among researchers community. During last two decades, this act has been highlighted that the physical and the chemical properties of nano-TiO_2 depend on its size, morphology and crystalline polymorph strongly [8].

Crystallization is a process that nucleat and grow particles to form structures [8]. It plays an important role in determining the crystal structure, shape, size and size distribution of the nanomaterials. Instead of nanoparticles [6, 9, 10], there are several nanostructures, such as nanowires (NWs) [11-14], nano-flakes [15], nanorods [16], nanobelts [17], nanorings [18], nanocables [19], nanotubes [20, 21], nanocolumns [22], nanocombs [23] and nanoneedles [24]. Therefore, a greater control over the size, shape, and composition of nanocrystals by understanding the theoretical approach about the mechanism of nanocrystal formation is able to tune the abovementioned properties. There have been reported that the differences being attributed to variations in the stoichiometric of the synthesis, the impurities content, the crystalline size and the type of electronic transition [25] especially in sol-gel method.

Sol-gel is one of the bottom-up approaches used to synthesis nano-scale materials [6, 9, 10, 15, 26, 27] which has notable advantages. It is made up of solutions then lead to a solid phase without a precipitate [28]. The use of sol-gel method in the latest nano - field is due to its low cost process [14]without involving any expensive machines compared to solid state processing routes using ball milling [29-31] and RF magnetron sputtering [32, 33]. Besides that, it can be done under ambient temperature which is low temperature processing and it synthesis high homogeneity and purity [10, 34, 35] of the nanostructures. Besides synthesis product in a batch form, it also represents nanotechnology; where it becomes interesting when used in nano-sized TiO_2 preparation [36, 37]. In sol-gel process, a synthesized precursor solution can be applied for film deposition purpose using various approaches like spin-coating and dip-coating techniques. Moreover, further condense the prepared solution make it slowly change to gel-like and this can produce dense ceramic or powders. Typically, the sol-gel derived precipitates are amorphous in nature. Therefore, it is required for further heat treatment to induce crystallization. The heat applied is able to improve the structural order between Ti-and-O due to the total elimination of organic compounds also lower defect density of the films. Besides that, this annealing effect can improve the adhesion layer between the deposited film and substrate. This condition will lead to variation in the microstructural properties of the TiO_2. Besides annealing temperature control, there are several parameters for controlling the sol-gel process to prepare TiO_2 particles with significant properties like precursor's concentration of precursor titanium alkoxide. It has been demonstrated that this parameter also gives big impacts on the crystallization behavior and the characteristics of the final particle. The size, stability, and morphology of the sol produced from alkoxide is strongly affected by the hydrolysis and pH. The pH of the prepared solution has a great influence on the final size and crystalline phases growth of TiO_2 nanoparticles [34]. The reaction morphology and the effect of the pH on the formation of TiO_2 particles is of great interest, because

nanosized particles are formed under these conditions [34]. Thus, a controlled on pH and reaction morphology are required for the optimization of the preparation conditions of TiO_2.

A TiO_2 solution is very unstable in the neutral pH range and therefore it easily agglomerates when it transforms into the gel state [34]. Moreover, its electrical properties are unstable and it is a modest semiconductor and a mediocre insulator. However, the existence of acid or base is more favorable in order to control stability of the TiO_2 solution. For the electrical conductivity, the principal factors are influenced by the concentration and nature of the chemical impurities incorporated in TiO_2, and the morphology of the thin films. Thus, the objectives of this research are to study the effect of TiO_2 morphology and crystalline structures instead of electrical properties when different pH of TiO_2 solution was despersed via sol-gel method by varying the stabilizers used.

2. METHODOLOGY

The p-type silicon substrate with <1 0 0> orientation was cleaned using RCA1, RCA2 and hydrofluoric acid (HF) to remove native oxide and small particles. RCA1 solution was prepared by mixing of DI water, ammonium hydroxide [NH_4OH(27%)], and hydrogen peroxide [H_2O_2 (30%)] by maintaining the ratio of 5 : 1 : 1. For the RCA2 preparation, hydrochloric acid [HCL (27%)] and hydrogen peroxide [H_2O_2 (30%)] were mixed in DI water by maintaining the composition at 6 : 1 : 1. The residual oxide layer was removed by dipping the substrate into a BOE solution followed by washing with DI water and drying under N_2 flow. After the cleaning process, the silicon wafer was thermally oxidized to generate a 150 nm layer of SiO_2. The oxide layer is used to isolate the deposited TiO_2 film from silicon substrate in order to neglect the influence of current flow from silicon substrate.

After thermally oxidized; ethanol 96%, titanium isopropoxide ($Ti[OCH(CH_3)_2]_4$, 97%) and acetic acid (AA) were mixed with 9:1:0.1 ratios under magnetic stirrer with speed 1000 rpm at 85^oC within 1 h. Ethanol as a solvent, tinium isopropoxide (TIP) as a precursor and AA as a stabilizer. Another two new TiO_2 solutions were prepared by changing the stabilizer used to hydrochloric acid (HCl) and monoethanolamine (MEA). The chemicals involved have been shown in Table 1.

Table 1. The chemicals used to prepare TiO_2 films.

Solvent	Stabilizer	Precursor
Ethanol	Acetic acid (AA)	Titanium isopropoxide (TIP)
Ethanol	Hydrochloric acid (HCl)	Titanium isopropoxide (TIP)
Ethanol	Monoethanolamine (MEA)	Titanium isopropoxide (TIP)

Then the TiO_2 prepared solutions were deposited on selected substrates at a spin speed of 3000 rpm for 30 s. The coated films then were dried on hot plate at 90^oC for 15 min. After completing five

times spin-coating of TiO_2, the films were annealed at 400, 500, 600, 700 and 900 ^oC for 30 min. Finally, aluminum (Al) metal was deposited and using a conventional lithography process, an IDE device of 8.75 mm X 5.00 mm in size was fabricated on the SiO_2/Si substrate for electrical measurement purpose [38]. Fig. 1 shows the design of the fabricated device and it was probed with Keithley6487 picoammeter.

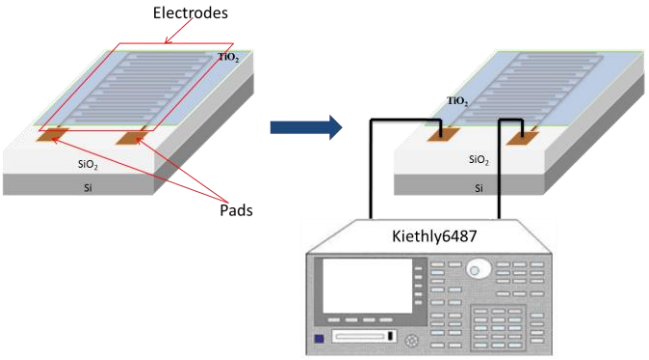

Figure 1. The TiO_2 thin film-based Al interdigitated electrodes with picoammeter.

The completed samples were then characterized to determine its properties. The PANalytical X-Pert Pro X-Ray Diffraction (XRD) using Ni-filtered CuKα radiation was perfomed at room temperature to investigate the crystallographic structures and phases. The morphology of coated TiO_2 thin films were characterized by HITACHI SU8020 Field Emission Scanning Electron Microscopy (FESEM) with 100k magnification and Atomic Force Microscopy (AFM) SII Sciko Instrument INC SPI3800N Probe station. Then the electrical characterization was carried out using Kiethly6487 picoammeter interface with Labtracer2.0 software. It was conducted by simply probe the needles at both pads and once the voltage was applied towards the device, currents value were come out as the output (see Fig. 1).

3. RESULTS AND DISCUSSION

The preparation of the TiO_2 thin films in the nanometer range of particles can be effectively conducted through the hydrolysis and condensation of titanium alkoxides in aqueous media. Synthesis TiO_2 solution via sol-gel method is usually prepared by the reactions of hydrolysis and polycondensation of titanium alkoxide, $(TiOR)_n$ to form oxopolymers, which are transformed into an oxide network. These reactions can be schematically represented as follows:

Hydrolysis

$$Ti(OR)_4 + 4H_2O \rightarrow Ti(OH)_4 + 4ROH \quad (1)$$

Condensation

$$Ti(OH)_4 \rightarrow TiO_2 \cdot xH_2O + (2\text{-}x)H_2O \quad (2)$$

where R is i-propyl.

Alkoxide were hydrolyzed when there was peresence of water. The tetravalent cations which were formed during hydrolysis were too acidic so that the nucleation of the stable hydroxide Ti(OH) cannot occur. Water molecules formed according to reaction (2) always bear a positive partial charge. There is oxolation and olation process during nucleation and growth. Then it leads to an amorphous oxide $TiO_2 \cdot nH_2O$ where the number n of water molecules depends on the experimental conditions. Different solvents used for TiO2 preparation caused the viscosity of the solutions were varied. This parameter gave a huge change towards the morphological and electrical properties of the TiO2 film. The TiO_2 solution with HCl stabilizer was synthesized with the lowest viscosity while the monoethanolamine stabilizer produces the highest viscosity of TiO_2 solution. Confirmation of TiO_2 crystalline phases and sizes can be seen in XRD result.

The XRD pattern of the as-prepared sample confirmed the existence of pure TiO_2 with different phases. The crystallographic planes of the XRD spectra were indexed using Bragg's law for XRD compared with JCPDS file No. 21-1272 for anatase [5] and JCPDS file No. 21-1276 for rutile phase [5]. Fig. 2, 3 and 4 show typical XRD patterns of the as-deposited and annealed TiO_2 films at various temperatures and effect on particle sizes and phases formed on different stabilizers used, which are HCl, AA and MEA in solution TiO_2 were discussed. There are both anatase and rutile phases exist without any amorphous crystal for these three TiO_2 thin films.

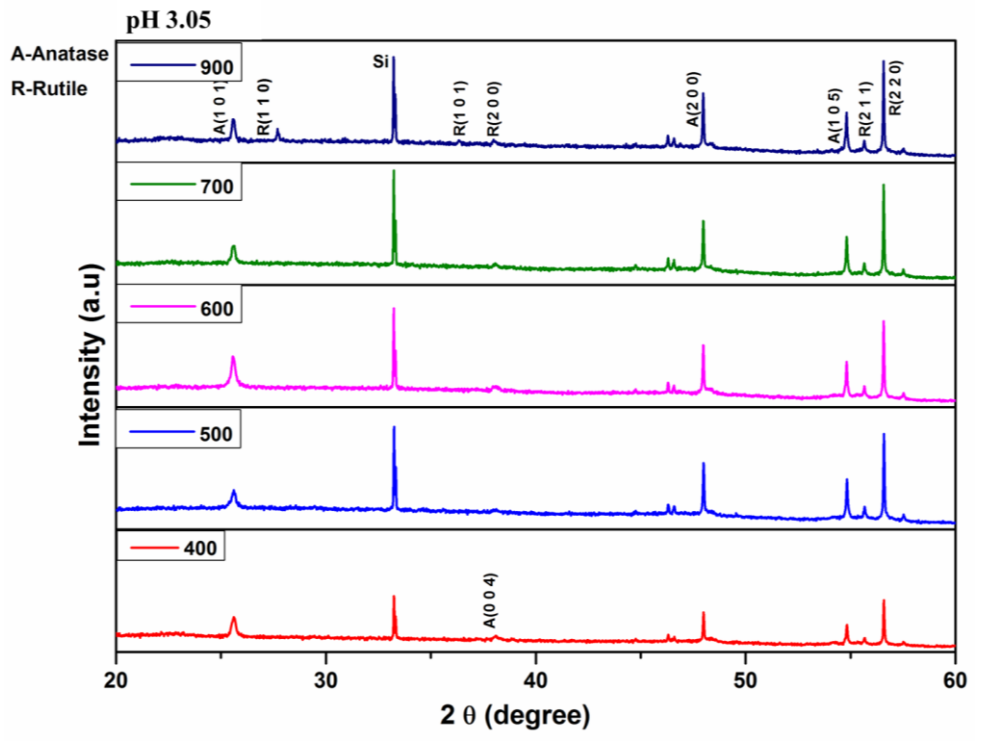

Figure 2. XRD images of TiO_2 thin film with AA stabilizer in TiO_2 solution synthesis by sol-gel method.

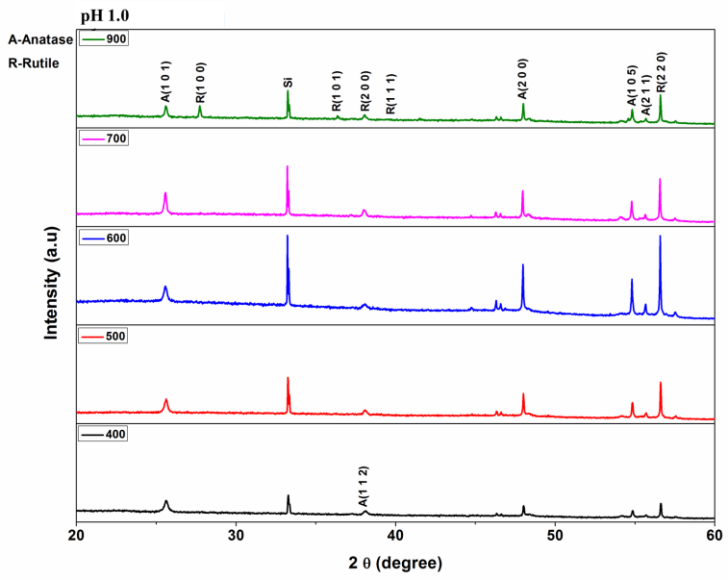

Figure 3. XRD images of TiO_2 thin film with HCl stabilizer in TiO_2 solution synthesis by sol-gel method.

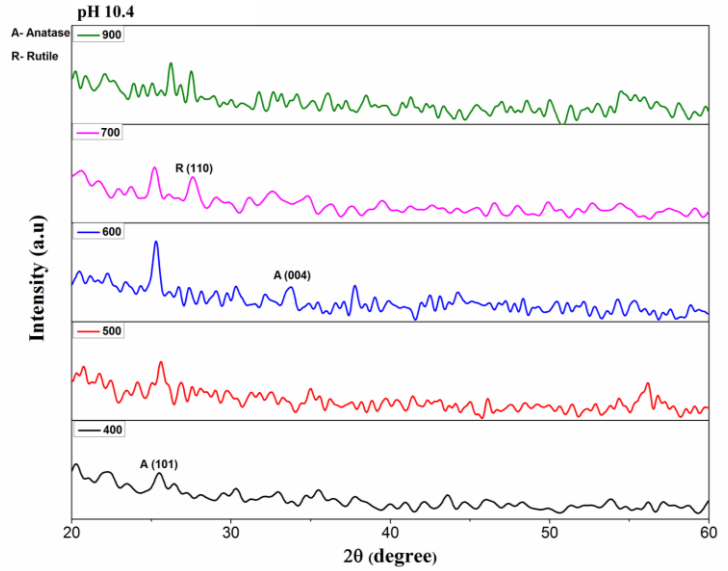

Figure 4. XRD images of TiO_2 thin film with MEA stabilizer in TiO_2 solution synthesis by sol-gel method.

Fig. 2 exposes XRD patterns of TiO_2 annealed for 30 min at 400, 500, 600, 700 and 900 ^oC with HCl (pH 1) as stabilizer. The representative (2 0 0) plane diffraction peak at $2\theta = 48.01^o$ is for anatase phase while (2 2 0) orientation at $2\theta = 56.61^o$ is for rutile. This obviously shows that the anatase and rutile phases occur even at very low temperature 400 ^oC without any amorphous phase growth. Fig. 3 reflects the XRD patterns of TiO_2 particles with AA (pH 3.05) as stabilizer calcined at 400, 500, 600, 700 and 900 ^oC. The results are slightly the same with HCl peaks where both anatase and rutile peaks can be observed at 400 ^oC without any phase transformation to rutile completely. Compared to the XRD peaks of the as deposited and annealed TiO_2 particles with MEA (pH10.4) stabilizer, the anatase (1 0 1) peak at $2\theta = 25.6^o$ can be seen above 400 ^oC and rutile (1 1 0) peak at 2θ

= 27.7^o can be seen above 700 ^{o}C in Fig. 4. There only the most intense peaks can clearly observed through this spectra results due to the existance of noise; where other peaks could not be detected since they were below the noise level.

Due to these results, peaks for HCl and AA are more favorable for the formation of rutile phase than MEA at the same concentration. This is in good agreement with Ahmadi et.al., [5] who study the the formation of TiO_2 nanoparticles with different parameters. This rare situation occurs due to the remaining amount of anatase became very small in the acid solution, because the phase transformation from anatase to rutile was significantly activated in the acid solution an increasing temperature [34]. Besides that, it is attributed to the high surface energy of the particles in strong acid. Moreover, the most intense peak for these low pH levels indicates to rutile with orientation (2 2 0). For the MEA stabilizer, the number of peaks and its intensity were slightly small. These are due to existence of noise; where other peaks could not be detected since they were below the noise level. This noise is possibly due to the thickness of coated TiO_2 film is too thin. However, there are similarity trends of peaks intensity decreased with temperature among these three catalysts used. The increment of peaks diffraction intensity with the annealing temperature increases up to 600 ^{o}C, implying an improvement in crystallinity. Otherwise, the reduction of intensity at higher temperature ($\geq$700 ^{o}C) exhibit abrupt transformation of anatase to rutile peak; where we can see more rutile peaks occur at higher temperature.

When the temperature was raised, the anatase phase transformed to the rutile phase, which could be attributed to the thermally promoted crystallite growth. In particular, the phases transformation were significantly activated by the HCl stabilizer. On the other hand, the phase transformation and the crystallization of the particles were not activated by the MEA (high pH level) stabilizer. This reveals that nucleation and growth of the rutile phase have been initiated at low temperatures somewhere from 400-600 ^{o}C with HCl and AA (low pH level) as the stabilizers. Thus, it may be assumed that the growth of rutile crystallization was affected by the pH of acid [34].

The estimated crystallite sizes perpendicular to the most intense reflection TiO_2 anatase planes from the full-width-half-maximum of the peak were measured through the Scherrer equation;

$$r = 0.9 \lambda / B \cos \theta \quad (3)$$

where λ is the X-Ray radiation, B is the full width at half-maximum (FWHM) of the diffraction peak.

From this calculation, the average sizes of rutile in pH 1 annealed at 400-600 ^{o}C are ~12.8 nm while the rutile obtained at pH 3.05 is ~ 17.7 nm and the antase obtained at pH10.4 is ~22.0 nm. Table 2 reflects the effect of stabilizers and the pH difference of TiO_2 solutions prepared by sol-gel method on the morphology and crystalline structure of the TiO_2. The HCl, AA and MEA as catalysts used in TiO_2 solution preparation via sol-gel method synthesis nanoparticles with various sizes. Therefore, the nucleation and growth of TiO_2 nanoparticles with rutile peaks can synthesized above 300 ^{o}C in the acid solution with small particles sizes and only at 700 ^{o}C rutile nanoparticles can be growth for base solution with bigger particles size. These crystallite size growth can be further conformed by the FESEM images shown below.

Table 2. Effect of different catalysts and pH on the morphology and crystalline structure of the TiO_2.

Stabilizer	pH	300 °C	400 °C	500 °C	600 °C	700 °C	900 °C	Particle size (nm)
		Crystal structure						
HCl	1	A+R	A+R	A+R	A+R	A+R	A+R	~12.8
AA	3.05	A+R	A+R	A+R	A+R	A+R	A+R	~17.7
MEA	10.4	-	A	A	A	A+R	A+R	~22.0

Fig. 5 shows FESEM nanographs of TiO_2 thin film prepared by mixing of HCl with TIP and the deposited film were annealed at 400, 500, 600, 700 and 900 °C. The morphology of annealed TiO_2 films are shown in Fig. 5 reveals the presence of numerous TiO_2 particles with diameters are about 23-87 nm. From 400 to 500 °C, the particles size are obviously shows a decrement in size. Then it increases with temperature increment.

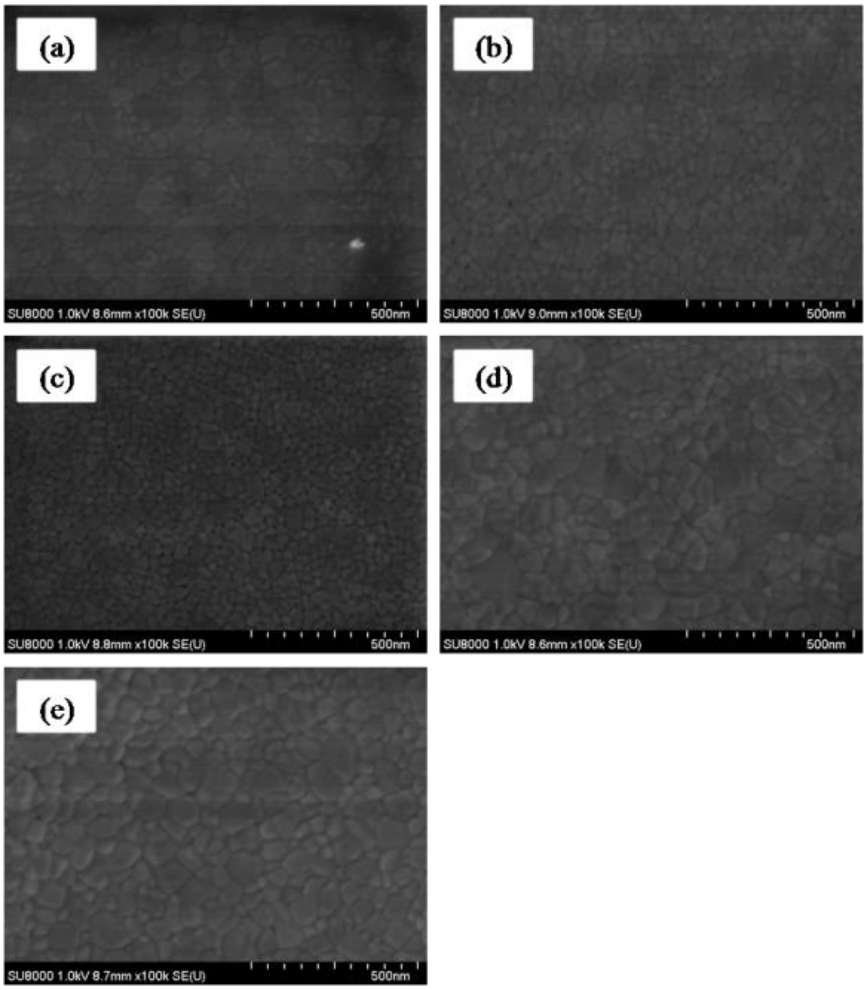

Figure 5. FESEM images of TiO_2 thin film heat-treated at (a) 400, (b) 500, (c) 600, (d) 700 and (e) 900 °C within 30 min with HCl stabilizer.

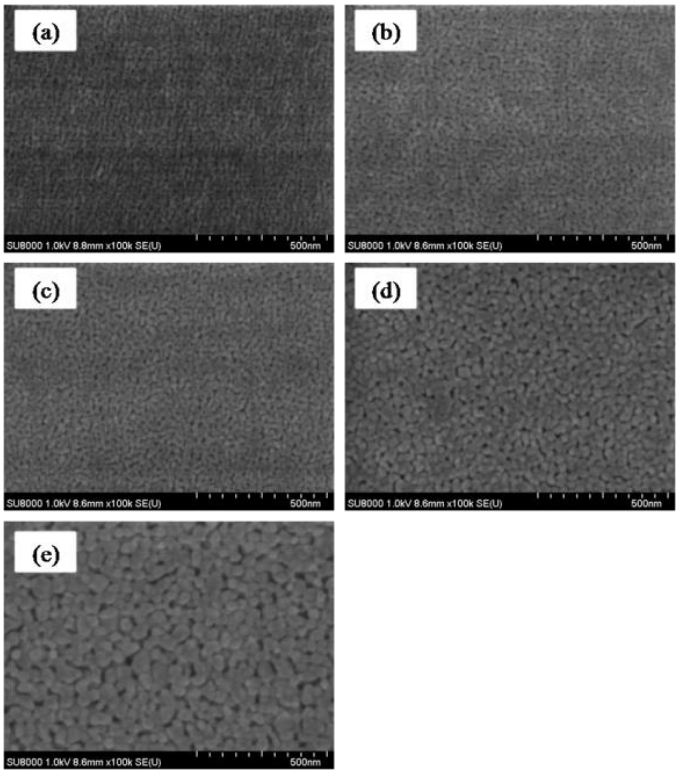

Figure 6. FESEM images of TiO_2 thin film heat-treated at (a) 400, (b) 500, (c) 600, (d) 700 and (e) 900 ^{o}C within 30 min with AA as stabilizer.

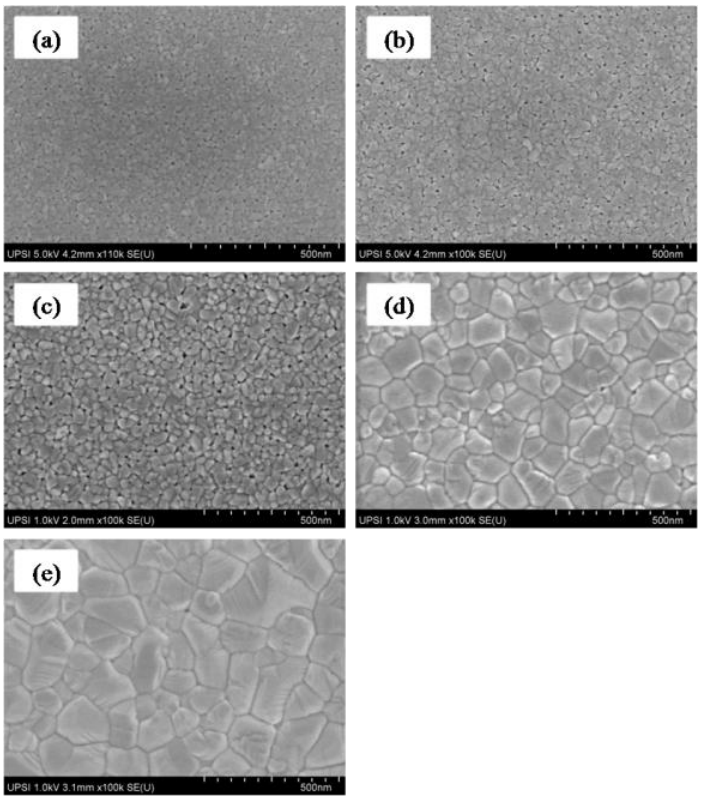

Figure 7. FESEM images of TiO_2 thin film heat-treated at (a) 400, (b) 500, (c) 600, (d) 700 and (e) 900 ^{o}C within 30 min with MEA as stabilizer.

On the other hand, Fig. 6 exposes FESEM images of TiO_2 thin films calcined at 400, 500, 600, 700 and 900 ^oC with AA as stabilizer. The average particles size are from 11.9 to 61.5 nm. While Fig. 7 exhibits the FESEM nanograph of TiO_2 film synthesis by sol-gel method which used MEA with TIP for hydrolysis process. The average crystallite size growth during these applied temperature are from 15 to 150 nm. Refering to the FESEM image in Fig. 5, 6 and 7, particles growth at 600 ^oC reflects the best crystalinity regarding to the crystal size and the uniformity of nucleation are good enough for future application which is UV-sensor [39].

Highly crystallined TiO_2 nanoparticles could be grown on a SiO_2 substrate with various diameters depending on the selected stabilizer. The effect of pH on the TiO_2 nanoparticles heat-treated at 600 ^oC was evaluated for the crystalline phase and size. The TiO_2 particles growth exhibited a homogeneous spherical morphology. When the stabilizer used is HCl with the pH 1, the particles growth with 15.90 nm in diameter and both anatase and rutile phases were observed. Otherwise, when the stabilizer is AA in the solution with pH 3.05, an increasing of particles size to 20.90 nm was measured but the morphology growth was slightly the same with HCl. However, when the pH of prepared TiO_2 solution was increased to pH 10.4 as MEA was used as catalyst, the particles growth were abruptly increase to 39.70 nm while maitaining the particles morphology when the growth was carried out at 500 ^oC for 30 min. These measured crystalline size are in good agreement with the calculated values using the Sherrer's equation. Moreover, this inspections demonstrated that the nanoparticles grew all over the substrate with uniform morphology. The presence of acid results in decreasing TiO_2 crystal size [5]. Thus, these results follow the trend where particles increased as the pH was increased from pH 1, pH 3.05 and pH 10.4. Therefore, the particles with same morphology and crystal structures were synthesized by the hydrolysis reaction of TIP using stabilizer with various pH values in acid and base solutions. The sizes and phase transformation of TiO_2 prepared by hydrolysis of TIP were strongly influenced by the presence of the stabilizers HCl, AA and MEA. Instead of that, nearly uniform thickness is an important criteria to obtain good cells with high efficiency [40].

The confirmation of the crystallization process studies by XRD and FESEM was carried out by AFM observation. Regarding the FESEM images, only the particles growth at 600 ^oC shows the best crystallization process, thus an image of AFM was selected for each stabilizer. These images show the spherical grains and different thickness of each TiO_2 thin film with different catalysts used. This is in good agreement with Naceur et al. [41] and Çörekçi et al. [42]. The formation of the grain sizes and morphology were controlled by the nucleation and growth procedures of TiO_2 nanoparticles which strongly related to the pH in TiO_2 solution synthesized. At pH 10.4, the crystallites are found to be sphere-shaped and relatively rough while a granular and elongated morphology starts to appear on the deposited TiO_2 thin film with HCl and AA as stailizers. As shown in Fig. 8 (a) and (b), we demonstrate that pH of the TiO_2 solutions decreases improve the crystallinity of the films and decrease the crystallites size as obtained from XRD and FESEM analysis. This elongated growth is due to the rutile phase occurs [41] at these TiO_2 films annealed at 600 ^oC for 30 min.

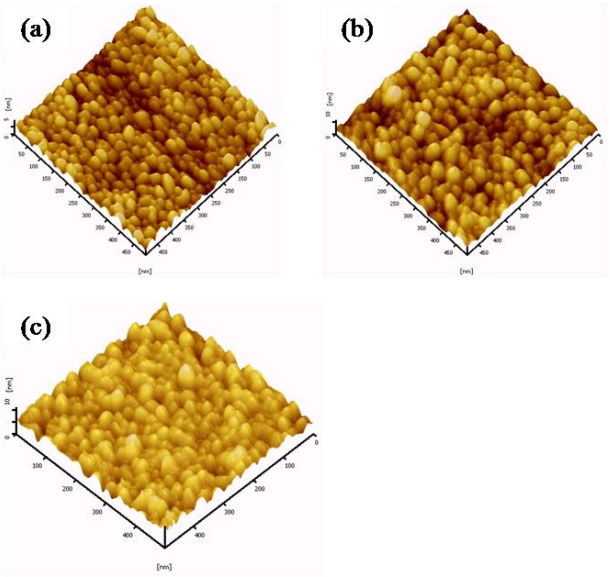

Figure 8. The AFM images of TiO_2 films with (a) HCl, (b) AA, and (c) MEA as stabilizers annealed at 600 ^oC.

On the other hand, the thickness of annealed TiO_2 thin films were increased with the grain size increment [42]. This increment is inrelation with the root mean square (RMS) surface roughness of the TiO_2 thin films [42]. It was find out the RMS were slowly increase from 1.2 nm, 1.3 and 2.1 nm when the the thickness of the film increases from 5, 10 to 20 nm respectively. Based on these results, it can be concluded that the reason of the increase of the films roughness, is due to the plenty existance of rutile phase and the growth of grain size. It also clearly shows that there is a remarkable change in surface morphology and roughness of the TiO_2 films depending on the film thicknesses [42].

Fig. 9 shows the current-voltage I–V characteristic, of n-type semiconducting TiO_2 thin films measured at room temperature, when as-deposited on p-type silicon. The direct current (DC) electrical measurements were taken in room temperature from a number of samples ($Al/TiO_2/SiO_2$) of different pH level from pH 1, pH 3.05 and pH 10.4.

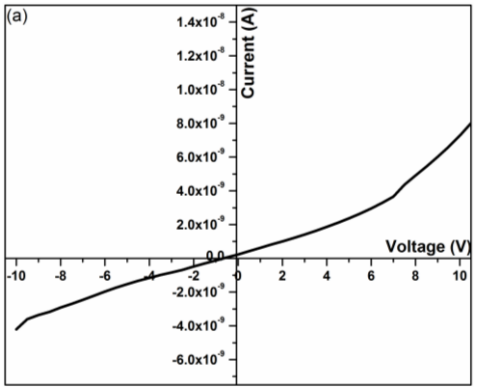

Figure 9. (a) The I-V curves of TiO_2 nanoparticles for (a) pH 1 TiO_2 solution.

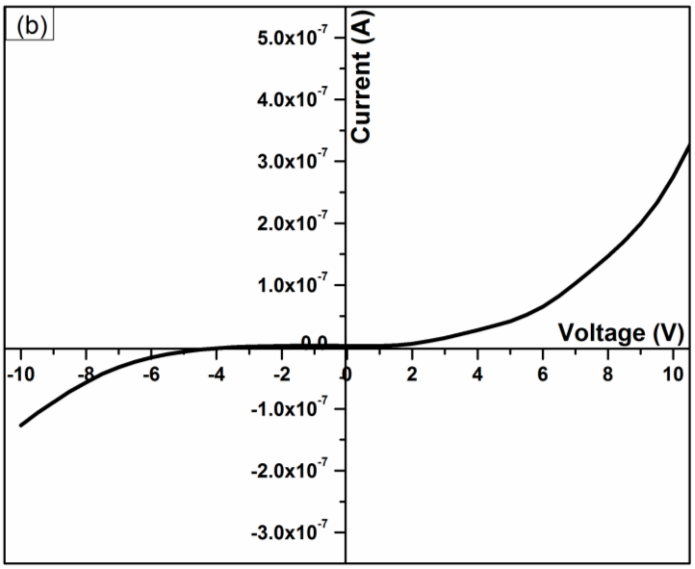

Figure 9. (b) The I-V curves of TiO_2 nanoparticles for (b) pH 3.05 TiO_2 solution.

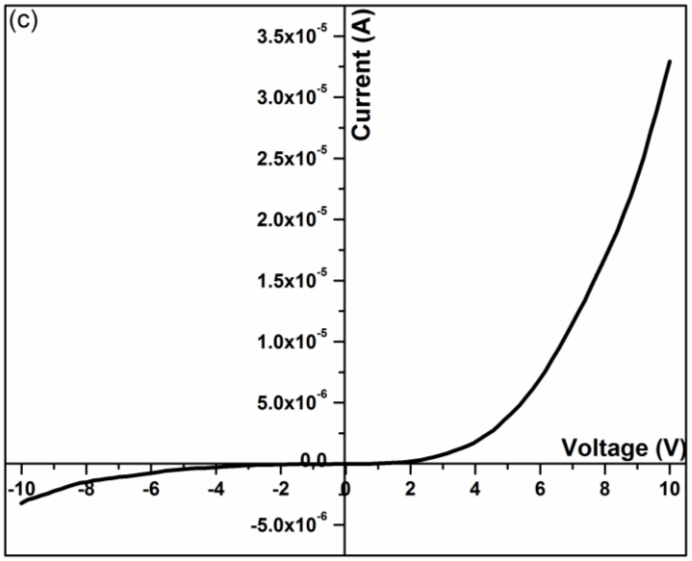

Figure 9. (c) The I-V curves of TiO_2 nanoparticles for (c) pH 10.4 TiO_2 solution.

The thickness of the metal (Al) coating on top of the TiO_2 layer was about 160 nm, prepared at a rate of deposition of 0.1 nm/s of vacuum background pressure of 2×10^{-5}mbar. The active area of the devices (W x L) was approximately 20.25 mm^2. Picoammeter was used to characterize the electrical properties of the TiO_2 thin films which synthesis with different stabilizers. Each I-V curve demonstrates rectifying behavior with a typical forward-to-reverse current ratio of 20 in the voltage of -10 to 10 V. The Schottky response may resulted from the large different of conduction band between Al metal and TiO_2. Since no tunneling effect occurs, an electron requires large energy to be excited from conduction band of Al to the conduction band of TiO_2 [43]. These results indicated that the change of the forward bias current under different condition is more obvious if compare to the reverse

bias current. Therefore, forward bias current is studied in this experiment. The result shows that the TiO_2 micro-gap device with HCl catalyst gives the lowest current (0.96 nA, 2V) in air condition then followed by 2.18 and 14.8 nA for pH 3.05 and pH 10.4, respectively. The current values are proportional with the applied pH level and deposited TiO_2 film thickness. At a fix temperature (600oC), the conductivity increases as a function of film thickness is increased. This is according to the oxygen content in the films equilibrates fast; thus the change in the conductivity is attributed to the change in the microstructure of the various films [44]. Instead of that, the efficiency of electrons accumulate at sharp point is much better than the other surfaces [45]. Thus heigh fluctuations on a rough surface would give adequate accumulation of charges and this leads to the appearance of local capacities on the rough surface [45].

4. CONCLUSIONS

In conclusion, TiO_2 nanoparticles with a homogeneous particle distribution were successfully prepared using a hydrolysis reaction of TIP. In future, the TiO_2 thin film with AA stabilizer will be used for biosensor application according to the electrical stability and surface roughness. While HCl stabilizer film is suggested for photosensor application since the shining effect and very smooth surface. However, MEA in TiO_2 thin film can only synthesis very well morphological properties instead of electrical properties which is not stable enough.

ACKNOWLEDGEMENTS
This research was supported by the Ministry of Higher Education Malaysia under Grant Nos. 901300001 and the author would like to thank Universiti Teknologi Mara (UiTM) for the XRD used, Universiti Pendididkan Sultan Idris (UPSI) and ADTEC Taiping for the FESEM used also all staff members of the Institute of Nanoelectronic Engineering in Universiti Malaysia Perlis (UniMAP) for their technical advice and contributions either directly or indirectly.

References

1. S. Nadzirah, U. Hashim, 2013 IEEE Regional Symposium on Micro and Nanoelectronics (RSM), 2013, p. 167.
2. S.S. Pradhan, S.K. Pradhan, V. Bhavanasi, S. Sahoo, S.N. Sarangi, S. Anwar, P.K. Barhai, *Thin Solid Films*, 520 (2011) 1809.
3. A. Moses Ezhil Raj, V. Agnes, V. Bena Jothy, C. Sanjeeviraja, *Materials Science in Semiconductor Processing*, 13 (2010) 389.
4. V. N. Koparde, P. T. Cummings, *ACSNano*, 2 (2008) 1620.
5. M. Ahmadi, M. Reza Ghasemi, H. Hashemipour Rafsanjani, *Journal of Materials Science and Engineerin*g, 5 (2011) 87.
6. S.N.S.A. Ayob, U. Hashim, IEEE International Conference on Biomedical Engineering and Sciences, 2012, p. 607.
7. A.-C. Lee, R.-H. Lin, C.-Y. Yang, M.-H. Lin, W.-Y. Wang, *Materials Chemistry and Physics*, 109 (2008) 275.
8. H. Mehranpour, M. Askari, M.S. Ghamsari, *Nanomaterials* (2011) 3.

9. S. Nadzirah, M. Kashif, U. Hashim, *Wulfenia*, 20 (2013) 253.
10. S. Nadzirah, U. Hashim, 2013 IEEE Regional Symposium on Micro and Nanoelectronics (RSM), 2013, p. 159.
11. S.M. Usman Ali, O. Nur, M. Willander, B. Danielsson, *Sensors and Actuators B: Chemical*, 145 (2010) 869.
12. M.H. Huang, Y. Wu, H. Feick, N. Tran, E. Weber, P. Yang, *Advanced Materials*, 13 (2001) 113.
13. S.N.S.A. Ayob, U.Hashim, IEEE International Conference on Biomedical Engineering and Sciences, 2012, p. 126.
14. S.N.S.A. Ayob, U. Hashim, IEEE International Conference on Semiconductors Electronics, 2012, p. 145.
15. M. Kashif, U. Ali, S. M., M.E. Ali, H.I. Abdulgafour, U. Hashim, M. Willander, Z. Hassan, *Physica status solidi* (a), 209 (2012) 143.
16. M. Kashif, U. Hashim, S.M.U. Ali, A.S. Ala'eddin, M. Willander, M.E. Ali, *Microelectronics International*, 29 (2012) 1.
17. Y.B. Li, Y. Bando, T. Sato, K. Kurashima, *Applied Physics Letters*, 81 (2002) 144.
18. W.L. Hughes, Z.L. Wang, *Applied Physics Letters*, 86 (2005) 043106.
19. S. Kim, M.-C. Jeong, B.-Y. Oh, W. Lee, J.-M. Myoung, *Journal of Crystal Growth*, 290 (2006) 485.
20. S.M.U. Ali, M. Kashif, Z.H. Ibupoto, M. Fakhar-e-Alam, U. Hashim, M. Willander, *Micro & Nano Letters*, IET, 6 (2011) 609.
21. X. Ren, C.H. Jiang, D.D. Li, L. He, *Materials Letters*, 62 (2008) 3114.
22. J.Y. Park, Y.S. Yun, Y.S. Hong, H. Oh, J.-J. Kim, S.S. Kim, *Composites Part B: Engineering*, 37 (2006) 408.
23. Y. Yang, B.K. Tay, X.W. Sun, Z.J. Han, Z.X. Shen, C. Lincoln, T. Smith, Nanoelectronics Conference, 2008, p. 20.
24. J. Zhang, Y. Yang, F. Jiang, J. Li, *Physica E: Low-dimensional Systems and Nanostructures*, 27 (2005) 302.
25. T. Guang-Lei, H. Hong-Bo, S. Jian-Da, *Chinese Physics Letters*, 22 (2005) 1787.
26. M. Kashif, Y. Al-Douri, U. Hashim, M.E. Ali, S.M.U. Ali, M. Willander, *Micro & Nano Letters*, 7 (2012) 163
27. K. Foo, U. Hashim, H. Prasad, M. Kashif, IEEE International Conference on Semiconductors Electronics, 2012, p. 191.
28. Y. Dimitriev, Y. Ivanova, R. Iordanova, *Journal of the University of Chemical Technology and Metallurgy*, 40 (2009) 181.
29. S. Chen, S. Zhang, W. Zhao, W. Liu, *Journal of Nanoparticle Research*, 11 (2009) 931.
30. M. Salari, M. Rezaee, S.M. Mousavi koie, P. Marashi, H. Aboutalebi, *International Journal of Modern Physics B*, 22 (2008) 2955.
31. S. Nadzirah, U. Hashim, *Advanced Materials Research*, 2014, p. 128.
32. C.H. Heo, S.-B. Lee, J.-H. Boo, *Thin Solid Films*, 475 (2005) 183.
33. S.J. Kang, K.J. Kim, M.C. Chung, S.C. Jung, S.I. Boo, S.K. Cho, W.J. Jeong, H.G. Ahn, J *Nanosci Nanotechnol*, 11 (1692) 1692.
34. C. Sung Lim, J. Ho Ryu, D.-H. Kim, S.-Y. Cho, W.-C. Oh, *Journal of Ceramic Processing Research*, 11 (2010) 736.
35. K.L. Foo, M. Kashif, U. Hashim, *Applied Mechanics and Materials* 284-287 (2013) 347.
36. N. Wetchakun, B. Incessungvorn, K. Wetchakun, S. Phanichphant, *Materials Letters*, 82 (2012) 195.
37. S. Nadzirah, U. Hashim, *Advanced Materials Research*, (2014) 124.
38. K. Foo, M. Kashif, U. Hashim, M. Ali, *Current Nanoscience*, 9 (2013) 288.
39. S.M. Nejad, S.G. Samani, E. Rahimi, 2nd International Conference on Mechanical and Electronics Engineering, 2010, p. V2.

40. M. Hamadanian, V. Jabbari, A. Gravand, *Materials Science in Semiconductor Processing*, 15 (2012) 371.
41. J. Ben Naceur, M. Gaidi, F. Bousbih, R. Mechiakh, R. Chtourou, *Current Applied Physics*, 12 (2011) 422.
42. S. Çörekçí, K. Kızılkaya, T. Asar, M. K. Öztürk, M. Çakmak, S. Özçelíkb, International Congress on Advances in Applied Physics and Materials Science, 2012, p. 247.
43. M.Z. Sahdan, M.S. Alias, N. Nafarizal, U. Hashim, IEEE International Conference on Semiconductors Electronics, 2012, p. 267.